Isothermal Crystallization Kinetics of High-Flow Nylon 6 by Differential Scanning Calorimetry

Fan Zhang, Li Zhou, Yuanqin Xiong, Guangpeng Liu, Weijian Xu

Department of Chemistry and Chemical Engineering, Institute of Polymer Research, Hunan University, Changsha 410082, People's Republic of China

Received 5 April 2008; accepted 21 August 2008
DOI 10.1002/app.29352
Published online 5 December 2008 in Wiley InterScience (www.interscience.wiley.com).

ABSTRACT: The isothermal crystallization kinetics have been investigated with differential scanning calorimetry for high-flow nylon 6, which was prepared with the mother salt of polyamidoamine dendrimers and *p*-phthalic acid, an end-capping agent, and ε-caprolactam by *in situ* polymerization. The Avrami equation has been adopted to study the crystallization kinetics. In comparison with pure nylon 6, the high-flow nylon 6 has a lower crystallization rate, which varies with the generation and content of polyamidoamine units in the nylon 6 matrix. The traditional analysis indicates that the values of the Avrami parameters calculated from the half-time of crystallization might be more in agreement with the actual crystallization mechanism than the parameters determined from the Avrami plots. The Avrami exponents of the high-flow nylon 6 range from 2.1 to 2.4, and this means that the crystallization of the high-flow nylon 6 is a two-dimensional growth process. The activation energies of the high-flow nylon 6, which were determined by the Arrhenius method, range from −293 to −382 kJ/mol. The activation energies decrease with the increase in the generation of polyamidoamine units but increase with the increase in the content of polyamidoamine units in the nylon 6 matrix. © 2008 Wiley Periodicals, Inc. J Appl Polym Sci 111: 2930–2937, 2009

Key words: crystallization; differential scanning calorimetry (DSC); kinetics (polym.)

INTRODUCTION

Over the past 2 decades, polyamidoamine (PAMAM) dendrimers have attracted more and more attention because of their unique features, such as three-dimensional architectures, low intrinsic viscosities, good solubility, and high reactivity due to the presence of a large number of terminal functional groups.[1–9] Because of the large number of amine end groups in PAMAM dendrimers, a kind of high-flow nylon 6 can be prepared by *in situ* polymerization.[10] In comparison with pure nylon 6, high-flow nylon 6 containing PAMAM units has high flow properties and almost the same mechanical properties.

It is well known to all that the physical, chemical, and mechanical properties of polymers depend on the morphology, crystal structure, and degree of crystallization. In practical processing, such as extrusion molding and film forming, crystallization often proceeds under isothermal and nonisothermal processes. To control the rate of crystallization and to obtain the anticipated morphology and properties, much research about the crystallization behavior and kinetics of polymers,[11–20] polymer mixtures,[21,22] and polymer composites[23–36] has been conducted during the past several decades. Generally, a sample is melted at or above the equilibrium melting point and is quickly quenched to the designated crystallization temperature (T_c).

To obtain materials with better physical properties, it is important to investigate the effect of PAMAM units in the nylon 6 matrix on the crystallization behavior and kinetics of the high-flow nylon 6 under isothermal conditions by differential scanning calorimetry (DSC).

EXPERIMENTAL

Materials

The high-flow nylon 6 was prepared with ε-caprolactam, an end-capping agent (acetic acid), and a mother salt solution of PAMAM dendrimers, *p*-phthalic acid, and distilled water by *in situ* polymerization.[10] The high-flow nylon 6 had a star structure and linear structure, as described in detail in a previous report.[10] Samples BPAG1*0.5, BPAG2*0.5, and BPAG3*0.5 contained 0.5 wt % generation 1 (G1), generation 2 (G2), and generation 3 (G3) PAMAM dendrimer units in a nylon 6 matrix, respectively. BPAG2*1.2 samples contained 1.2 wt % G2 PAMAM dendrimer units for comparative experiments with sample BPAG2*0.5. Sample LPA6 (pure nylon 6)

Correspondence to: W. Xu (weijxu_59@sina.com).

was also prepared under the same conditions for comparison.

DSC

Isothermal crystallization kinetics were carried out with a Q10-V9.4-Build 287 differential scanning calorimeter (TA Instruments, New Castle, DE); the temperature was calibrated with indium. All DSC was performed under a nitrogen atmosphere; the sample weights were between 5 and 7 mg.

Isothermal crystallization process

The isothermal crystallization and melting process of high-flow nylon 6 were performed as follows: the samples were heated to 250°C (at 20°C/min), kept there for 10 min to eliminate residual crystals, then cooled (at 100°C/min) to the designated T_c in the range of 187–190°C for isothermal crystallization for 30 min, and heated to 250°C at 20°C/min.

RESULTS AND DISCUSSION

Analysis of the thermograms

The isothermal thermograms from cooling at different temperatures for pure nylon 6 (LPA6) and high-flow nylon 6 (BPAG1*0.5, BPAG2*0.5, BPAG3*0.5, and BPAG2*1.2) are shown in Figures 1 and 2; the crystallization thermograms shift to longer times and become flatter with increasing T_c. These DSC crystallization thermograms indicate that the total crystallization time is lengthened and the crystallization rate decreases with increasing T_c, and this agrees with the kinetic theory of crystallization, according to which an increase in T_c will result in a decrease in supercooling and hence in a decrease in the growth rate.[37,38]

From the DSC digital information, plots of the relative crystallinity at crystallization time t [$X(t)$] for pure nylon 6 (LPA6) and high-flow nylon 6 (BPAG1*0.5, BPAG2*0.5, BPAG3*0.5, and BPAG2*1.2) at different values of t are presented in Figures 3 and 4, from which we can obtain the half-time of isothermal crystallization ($t_{1/2}$) when $X(t)$ is equal to 50%. The $t_{1/2}$ values of pure nylon 6 (LPA6) and high-flow nylon 6 (BPAG1*0.5, BPAG2*0.5, BPAG3*0.5, and BPAG2*1.2) are listed in Table I.

$t_{1/2}$ usually has an influence on the crystallization rate ($1/t_{1/2}$). The crystallization rate values are presented in Figure 5, which shows that the crystallization rate of pure nylon 6 is higher than that of high-flow nylon 6 at the same T_c values. Sample BPAG3*0.5 has a higher crystallization rate than BPAG2*0.5 but a lower crystallization rate than BPAG1*0.5 at lower T_c values. When T_c is above 188°C, sample BPAG3*0.5 has a higher crystallization rate than either BPAG1*0.5 or BPAG2*0.5. In addition, by comparing BPAG2*0.5 with BPAG2*1.2, we have found that the crystallization rate increases slightly with the increase in the content of PAMAM units in the nylon 6 matrix.

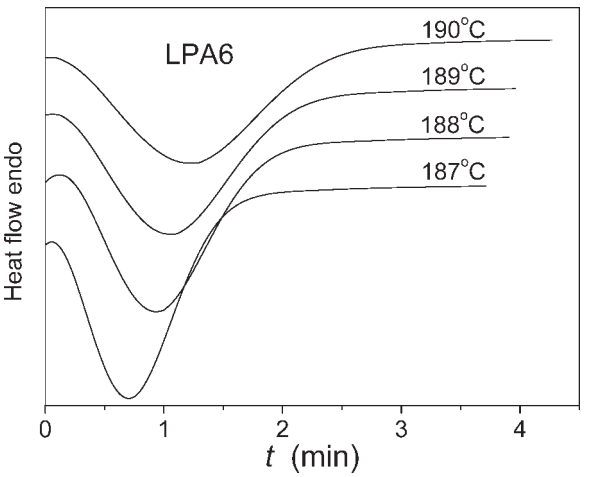

Figure 1 Heat flow versus time t during the isothermal crystallization of pure nylon 6 (LPA6) at different T_c's by DSC.

Figure 6 shows $X(t)$ of pure nylon 6 (LPA6) and high-flow nylon 6 (BPAG1*0.5, BPAG2*0.5, BPAG3*0.5, and BPAG2*1.2) at $T_c = 189$°C. It is easily found that, at the same T_c values, when $X(t)$ is 20–80%, (1) the crystallization rate of pure nylon 6 is higher than that of high-flow nylon 6, (2) sample BPAG3*0.5 has a higher crystallization rate than either BPAG1*0.5 or BPAG2*0.5, and (3) the crystallization rate increases slightly with the increase in the content of PAMAM units in the nylon 6 matrix. These conclusions are in agreement with the discussion on the crystallization rate.

The variation of the crystallization rates might be due to the presence of PAMAM units and *p*-phthalic acid in the nylon 6 matrix, which disturb the hydrogen bonds between neighboring molecular chains.[39] That is, the dendritic structure should weaken the hydrogen bonds between neighboring molecular chains and decrease the melting crystallization rate. The different generations or contents of PAMAM units in the nylon 6 matrix also have some influence on the melting crystallization process. Additionally, the PAMAM units of higher generations in the nylon 6 matrix might act more effectively as crystallization nuclei than those of lower generations.[37]

Traditional analysis based on the Avrami equation

The Avrami equation,[40,41] when used to describe the isothermal crystallization kinetics of a polymer, is expressed as follows:

$$1 - X(t) = \exp(-Kt^n) \quad (1)$$

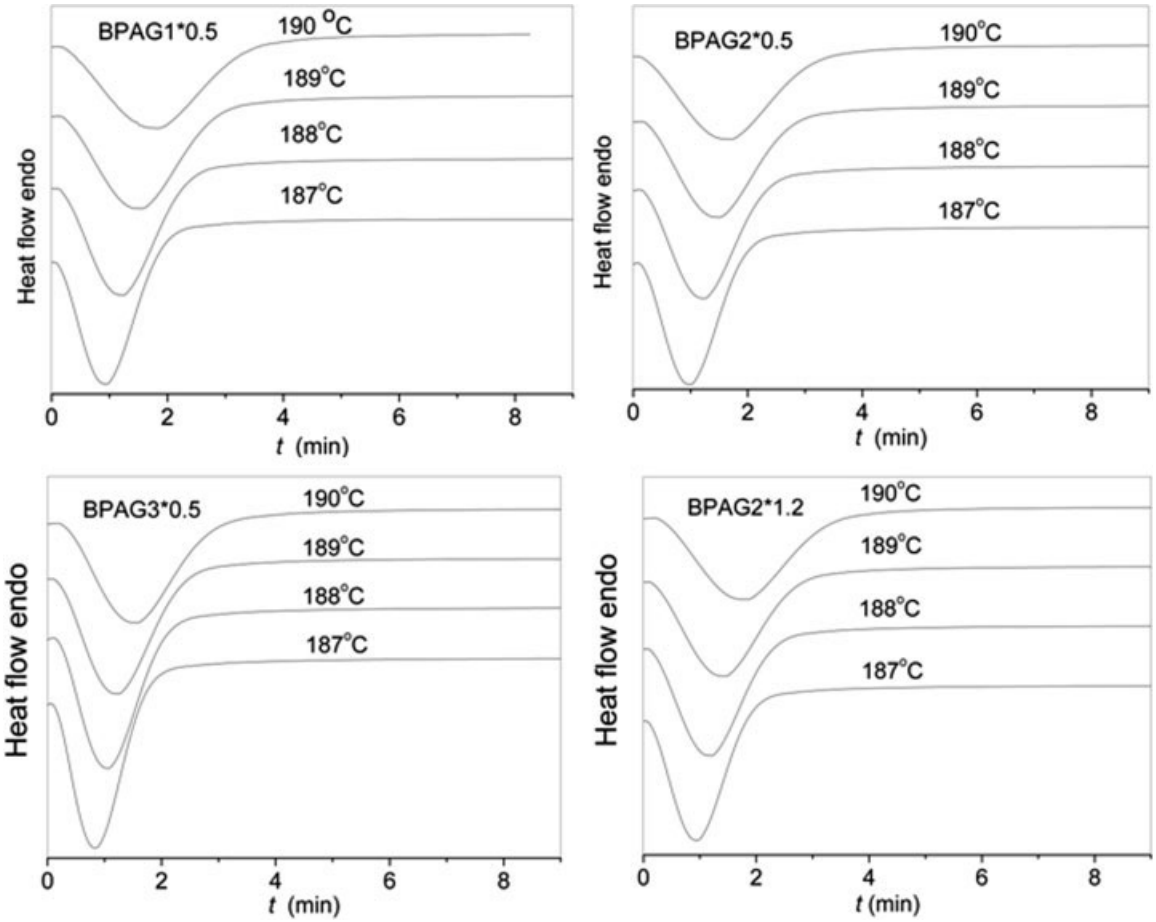

Figure 2 Heat flow versus time t during the isothermal crystallization of high-flow nylon 6 (BPAG1*0.5, BPAG2*0.5, BPAG3*0.5, and BPAG2*1.2) at different T_c's by DSC.

$$\lg[-\ln(1-X(t)] = \lg K + n \lg t \tag{2}$$

where n is the Avrami exponent and K is the crystallization rate constant. The double logarithmic plots of lg{−ln[1 − X(t)]} versus lg t are shown in Figures 7(a) and 8. As shown in Figure 7(b), the crystallization process is treated as a composite of three stages: (1) the buffer stage (considering the delay in the DSC signal under isothermal conditions[37]), (2) the primary crystallization stage, and (3) the secondary crystallization stage. It can be seen from Figure 7(b) that the Avrami plot in the primary crystallization stage shows good linearity. The parameters n and K are obtained through the fitting of the isothermal crystallization data to a linearized form of the Avrami plots in the primary crystallization stage. The other n and K values are obtained in the same way. All the n and K values are listed in Table I.

According to eq. (1)

$$\frac{\partial(1 - X(t))}{\partial t} = \frac{\partial(\exp(-Kt^n))}{\partial t} = -nKt^{n-1}\exp(-Kt^n) \tag{3}$$

Let

$$S = \frac{\partial(1 - X(t))}{\partial(\ln t)} = \frac{\partial(1 - X(t))}{\partial t} t \tag{4}$$

When $X(t) = 0.5$ and $t = t_{1/2}$, we have

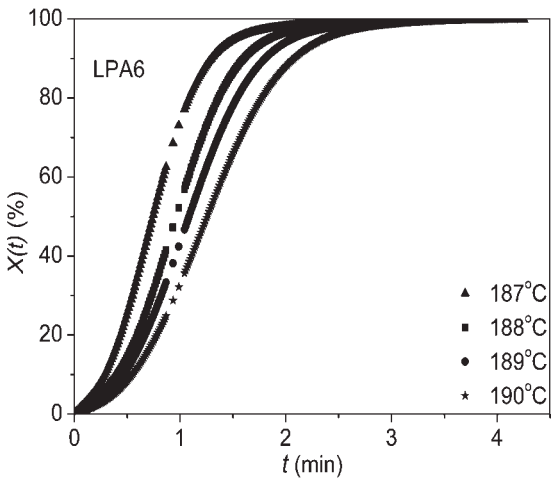

Figure 3 $X(t)$ versus time t in the process of isothermal crystallization of pure nylon 6 (LPA6).

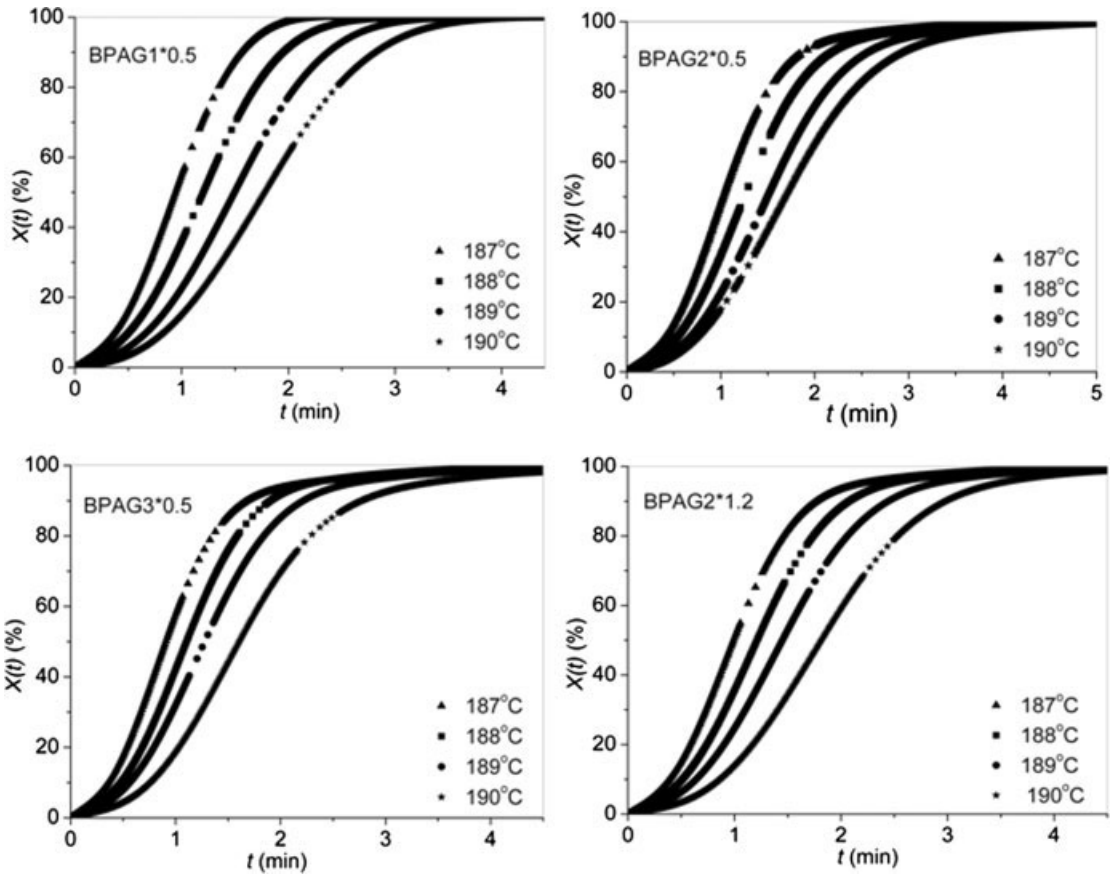

Figure 4 $X(t)$ versus time t in the process of isothermal crystallization of high-flow nylon 6 (BPAG1*0.5, BPAG2*0.5, BPAG3*0.5, and BPAG2*1.2).

TABLE I
Parameters of the Isothermal Crystallization of Pure Nylon 6 (LPA6) and High-Flow Nylon 6 (BPAG1*0.5, BPAG2*0.5, BPAG3*0.5, and BPAG2*1.2)

Sample	T_c (°C)	n^a	K^a	$S_{1/2}$	$t_{1/2}$ (s)	n^b	K^b	t_{max} (s)[c]	t_{max} (s)[d]	t_{max} (s)[e]
LPA6	187	2.33	1.5125	−0.778	44.58	2.25	1.3508	42.1	39.5	40.4
	188	2.33	0.9256	−0.851	57.80	2.46	0.7598	55.9	48.8	54.3
	189	2.36	0.6199	−0.844	65.09	2.44	0.5685	63.8	58.2	60.9
	190	2.31	0.4312	−0.857	75.33	2.47	0.3950	74.4	67.6	70.8
BPAG1*0.5	187	2.16	0.8958	−0.805	54.89	2.32	0.8523	54.0	47.3	50.4
	188	2.16	0.5330	−0.821	69.40	2.37	0.4911	70.4	60.2	64.3
	189	2.19	0.3299	−0.885	87.00	2.55	0.2685	90.5	75.4	82.7
	190	2.20	0.2162	−0.858	100.58	2.48	0.1930	103.4	91.4	94.6
BPAG2*0.5	187	2.24	0.7342	−0.799	61.6	2.31	0.6524	59.2	52.9	56.5
	188	2.28	0.4553	−0.852	75.9	2.45	0.3889	73.8	65.8	71.2
	189	2.20	0.3354	−0.851	90.0	2.52	0.2487	90.2	74.8	85.3
	190	2.29	0.2198	−0.855	101.5	2.46	0.1895	102.0	90.5	95.4
BPAG3*0.5	187	2.23	0.9913	−0.765	54.36	2.20	0.8618	50.1	46.1	48.7
	188	2.32	0.6100	−0.836	66.20	2.41	0.5468	62.6	58.2	61.7
	189	2.31	0.4284	−0.841	76.6	2.43	0.3831	73.4	67.7	71.6
	190	2.26	0.3203	−0.816	87.52	2.36	0.2848	84.6	76.7	80.9
BPAG2*1.2	187	2.21	0.7956	−0.778	59.42	2.24	0.7084	56.6	50.7	53.8
	188	2.24	0.4873	−0.826	72.67	2.38	0.4390	71.1	63.5	67.5
	189	2.20	0.3099	−0.854	86.93	2.47	0.2779	86.9	77.6	81.7
	190	2.21	0.2173	−0.815	96.49	2.35	0.2268	96.8	91.1	89.1

[a] Determined from the Avrami plots.
[b] Calculated from $t_{1/2}$.
[c] Determined from Figures 1 and 2.
[d] Calculated from the Avrami plots and with eq. (7).
[e] Calculated from $t_{1/2}$ and with eq. (7).

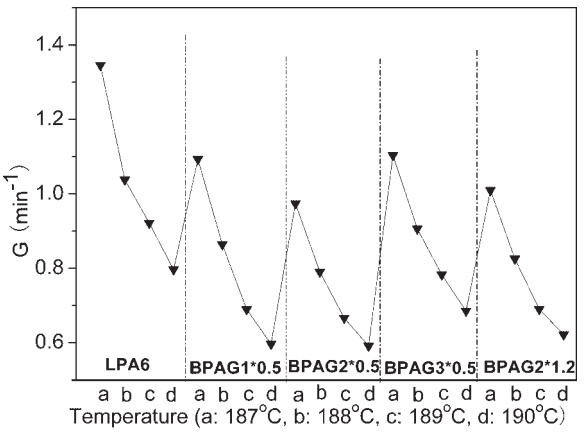

Figure 5 Crystallization rate (G) values of pure nylon 6 (LPA6) and high-flow nylon 6 (BPAG1*0.5, BPAG2*0.5, BPAG3*0.5, and BPAG2*1.2) at different T_c's.

$$K = \frac{\ln 2}{t_{1/2}^n} \tag{5}$$

$$S_{1/2} = -\frac{n \ln 2}{2} \tag{6}$$

Figure 9 presents a plot of $1 - X(t)$ versus ln t, showing a representative example of how to obtain the value of $S_{1/2}$. The values of $S_{1/2}$ are listed in Table I. Another set of n and K values were calculated from $t_{1/2}$ (Table I).

t_{max} represents the time required to reach the maximum rate of heat flow, and it corresponds to the changeover to a slower kinetic process due to the impingement of adjacent spherulites, Meanwhile, because t_{max} is the solution of $dH/dt = 0$, we can use the Avrami equation [eq. (1)] to derive t_{max} in terms of n and K:

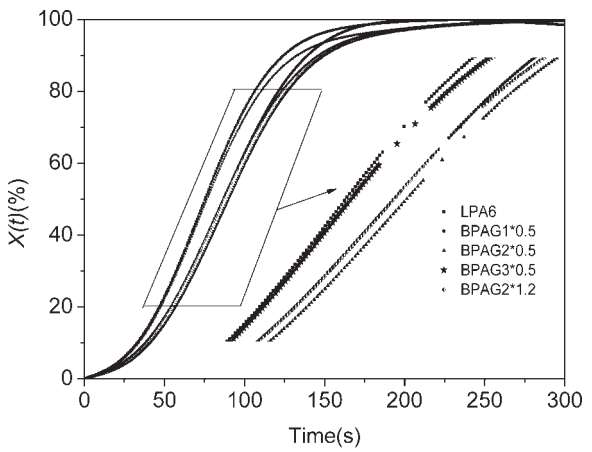

Figure 6 Plots of $X(t)$ versus time for pure nylon 6 (LPA6) and high-flow nylon 6 (BPAG1*0.5, BPAG2*0.5, BPAG3*0.5, and BPAG2*1.2) at $T_c = 189$°C.

$$t_{max} = \left[\frac{n-1}{nK}\right]^{1/n} \tag{7}$$

Two sets of n and K values, determined from the Avrami plots and from $t_{1/2}$, resulted in two sets of t_{max} values from eq. (7). Meanwhile, another set of t_{max} values were determined from Figures 1 and 2. The three sets of t_{max} values are all listed in Table I.

Table I shows that the t_{max} values obtained from Figures 1 and 2 are in agreement with the t_{max} values calculated from $t_{1/2}$. The two sets of t_{max} values become more similar with both the increase in the generation of PAMAM units and the decrease in T_c. However, the variation of t_{max} values is not obvious with the increase in the content of PAMAM units in the nylon 6 matrix. Moreover, it is easily found that the t_{max} values are more influenced by T_c than by the content or generation of PAMAM units in the nylon 6 matrix.

The results indicate that the t_{max} values calculated from $t_{1/2}$ are more similar to the actual t_{max} values obtained from Figures 1 and 2 than to those calculated from the Avrami plots and eq. (7). The causes

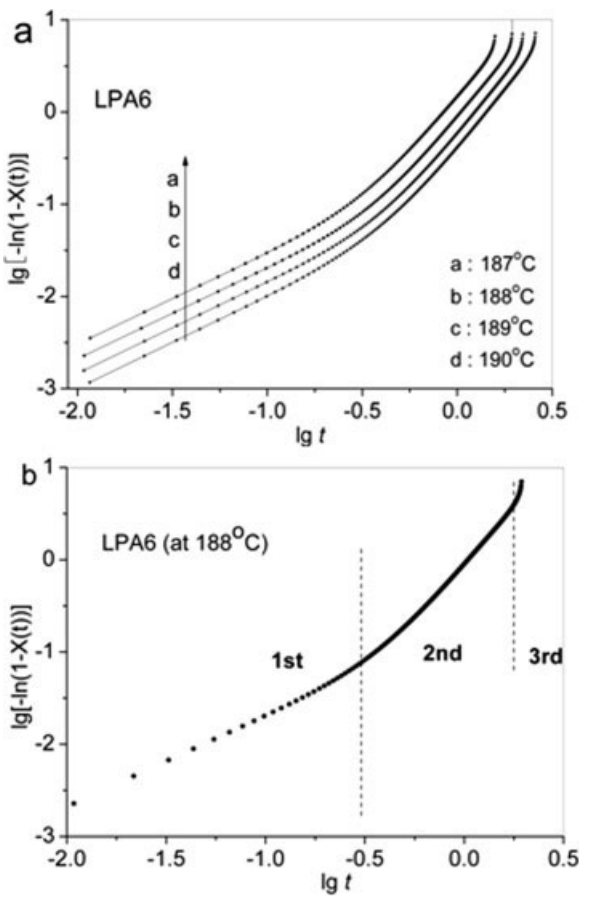

Figure 7 (a) Avrami plots of lg{−ln[1 − $X(t)$]} versus lg t for pure nylon 6 (LPA6) for isothermal crystallization at the indicated temperatures and (b) representative example of the linear fit of the Avrami plots.

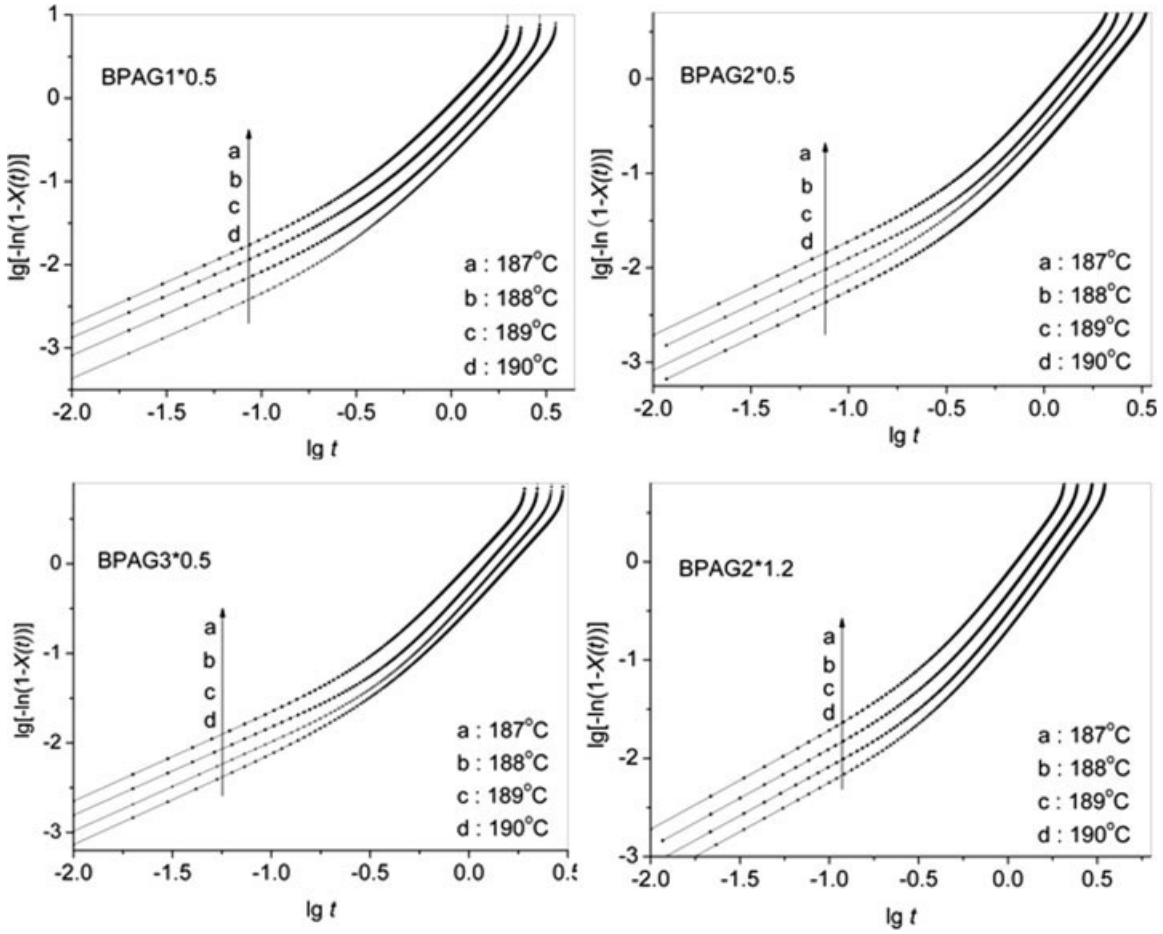

Figure 8 Avrami plots of lg{−ln[1 − X(t)]} versus lg t for high-flow nylon 6 (BPAG1*0.5, BPAG2*0.5, BPAG3*0.5, and BPAG2*1.2).

might be attributed to the delay in the DSC signal.[37] The results also imply that the values of the Avrami parameters calculated from $t_{1/2}$ might be more in agreement with the actual crystallization mechanism than that determined from the Avrami plots.

The n values for pure nylon 6 and high-flow nylon 6 range from 2.1 to 2.4, and this suggests that two-dimensional crystallization growth occurs under the experimental conditions.[11] According to Table I, the values of crystallization rate parameter K decrease

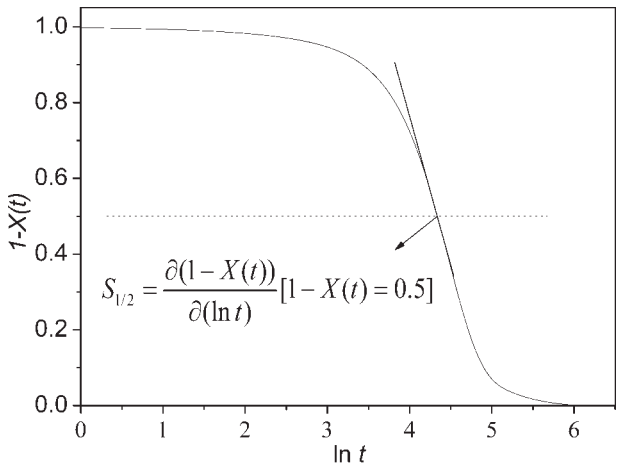

Figure 9 Representative example of a plot of 1 − $X(t)$ versus ln t.

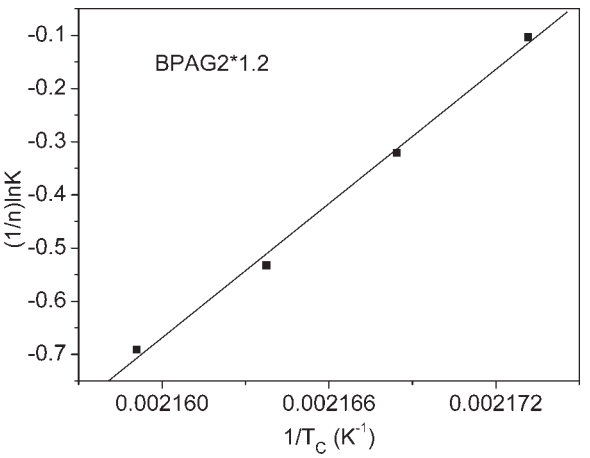

Figure 10 Plot of $(1/n)\ln K$ versus $1/T_c$ for sample BPAG2*1.2.

TABLE II
ΔE Values of Pure Nylon 6 (LPA6) and High-Flow Nylon 6 (BPAG1*0.5, BPAG2*0.5, BPAG3*0.5, and BPAG2*1.2)

Sample	LPA6	BPAG1*0.5	BPAG2*0.5	BPAG3*0.5	BPAG2*1.2
ΔE (kJ/mol)	−314.76	−381.18	−305.27	−293.07	−349.75

with the increase in T_c, and the K values of pure nylon 6 are larger than those of high-flow nylon 6. The K values of sample BPAG1*0.5 are larger than those of BPAG2*0.5 but lower than those of BPAG3*0.5. Moreover, the K values of sample BPAG2*1.2 are larger than those of BPAG2*0.5 at the T_c values of 187 and 188°C, but the reverse conclusion can be drawn at both 189 and 190°C. The variation of K is not completely in agreement with that of the crystallization rate.

Crystallization activation energy

The Avrami parameter K is assumed to be thermally activated and can be used to determine the crystallization activation energy. The crystallization rate can be approximately described by the following Arrhenius equation:[42]

$$K^{1/n} = K_0 \exp(-\Delta E/RT_c) \quad (8)$$

$$(1/n)\ln K = \ln K_0 - \Delta E/RT_c \quad (9)$$

where K_0 is a pre-exponential constant, R is the gas constant, T_c is the absolute crystallization temperature, and ΔE is the crystallization energy for the primary crystallization process. ΔE can be determined from the slope coefficient of plots of $(1/n)\ln K$ versus $1/T_c$. Figure 10 shows the linear relation plot of $(1/n)\ln K$ versus $1/T_c$ for sample BPAG2*1.2. The slope is equal to $d[(1/n)\ln K]/d(1/T_c) = -\Delta E/R = -42{,}062.26$ J/mol, and ΔE is −349.75 kJ/mol. The ΔE values of the other samples were also obtained in the same way (Table II).

Table II shows the variation of the activation energy of pure nylon 6 (LPA6) and high-flow nylon 6 (BPAG1*0.5, BPAG2*0.5, BPAG3*0.5, and BPAG2*1.2). It is easily found that the ΔE value of sample LPA6 is higher than those of sample BPAG2*0.5 and BPAG3*0.5 but lower than those of BPAG1*0.5 and BPAG2*1.2. Table II also indicates that the value of ΔE decreases with the increase in the generation of PAMAM units and increases with the increase in the content of PAMAM units. The PAMAM units of higher generations in the nylon 6 matrix act more effectively as nuclei, and this results in a decrease in the crystallization free energy barrier and thus a decrease in the crystallization activation energy.[37] The increase in the content of PAMAM units has a bad effect on the isothermal crystallization of high-flow nylon 6.

CONCLUSIONS

In comparison with pure nylon 6, high-flow nylon 6 has a lower crystallization rate, and the values of the crystallization rate vary with the generation of PAMAM units and increase slightly with the increase in the content of PAMAM units in the nylon 6 matrix. The t_{max} values obtained from plots of the heat flow versus time are in agreement with the t_{max} values calculated from $t_{1/2}$. The two sets of t_{max} values become more similar with both the increase in the generation of PAMAM units and the decrease in T_c. The traditional analysis implies that the values of Avrami parameters calculated from $t_{1/2}$ might be more similar to the actual crystallization mechanism than parameters determined from the Avrami plots. The n values of high-flow nylon 6 range from 2.1 to 2.4, and this means that the crystallization of high-flow nylon 6 is a two-dimensional growth process. The activation energies, which were determined by the Arrhenius method, vary within the range of −293 to −382 kJ/mol. The activation energies decrease with the increase in the generation of PAMAM units and increase with the increase in the content of PAMAM units in the nylon 6 matrix.

References

1. Fréchet, J. M. J. Science 1994, 263, 1710.
2. Fréchet, J. M. J.; Hawker, C. J.; Gitsov, I.; Leon, J. W. J Macromol Sci Pure Appl Chem 1996, 33, 1399.
3. Malmström, E.; Hult, A. J Macromol Sci Rev Macromol Chem Phys 1997, 37, 555.
4. Kim, Y. H. J Polym Sci Part A: Polym Chem 1998, 36, 1685.
5. Bosman, A. W.; Janssen, H. M.; Meijer, E. W. Chem Rev 1999, 99, 1665.
6. Inoue, K. Prog Polym Sci 2000, 25, 453.
7. Voit, B. J Polym Sci Part A: Polym Chem 2000, 38, 2505.
8. Jikei, M.; Kakimoto, M. Prog Polym Sci 2001, 26, 1233.
9. Gao, C.; Yan, D. Y. Prog Polym Sci 2004, 29, 183.
10. Zhang, F.; Zhou, L.; Liu, Y. C.; Xu, W. J.; Xiong, Y. Q. J Appl Polym Sci 2008, 108, 2365.
11. Ozawa, T. Polymer 1971, 12, 150.
12. Risch, B. G.; Wilkes, G. L.; Warakomski, J. M. 1993, 34, 2330.
13. Liu, T. X.; Mo, Z. S.; Wang, S. E.; Zhang, H. F. Eur Polym J 1997, 33, 1405.
14. Lorenzo, M. L. D.; Silvestre, C. Prog Polym Sci 1999, 24, 917.
15. Mandelkern, L.; Alamo, R. G.; Haigh, J. A. Macromolecules 1998, 31, 765.
16. Li, Y. J.; Zhu, X. Y.; Yan, D. Y. Polym Eng Sci 2000, 40, 1989.
17. Ren, M. Q.; Mo, Z. S.; Chen, Q. Y.; Song, J. B.; Wang, S. Y.; Zhang, H. F.; Zhao, Q. X. Polymer 2004, 45, 3511.
18. Yang, J.; McCoy, B. J.; Madras, G. J Phys Chem B 2005, 109, 18550.
19. Wang, L.; Dong, C. M. J Polym Sci Part A: Polym Chem 2006, 44, 2226.
20. Du, J.; Niu, H.; Dong, J. Y.; Dong, X.; Wang, D.; He, A.; Han, C. C. Macromolecules 2008, 41, 1421.

21. Hao, Q.; Li, F.; Li, Q.; Li, Y.; Jia, L.; Yang, J.; Fang, Q.; Cao, A. Biomacromolecules 2005, 6, 2236.
22. Long, Y.; Shanks, R. A.; Stachurski, Z. H. Prog Polym Sci 1995, 20, 651.
23. Wang, Z.; Jiang, B. Macromolecules 1997, 30, 6223.
24. An, Y. X.; Dong, L. S.; Xing, P. X.; Zhuang, Y. G.; Mo, Z. S.; Feng, Z. L. Eur Polym J 1997, 33, 1449.
25. An, Y. X.; Dong, L. S.; Li, L. X.; Mo, Z. S.; Feng, Z. L. Eur Polym J 1999, 35, 365.
26. Xu, J. T.; Fairclough, J. P. A.; Mai, S. M.; Ryan, A. J.; Chaibundit, C. Macromolecules 2002, 35, 6937.
27. Zhang, G. S.; Li, Y. J.; Zhu, X. Y.; Yan, D. Y.; Xu, Y. Y. Polym Eng Sci 2003, 43, 204.
28. Liu, M. Y.; Zhao, Q. X.; Wang, Y. D.; Zhang, C. G.; Mo, Z. S.; Cao, S. K. Polymer 2003, 44, 2537.
29. Fornes, T. D.; Paul, D. R. Polymer 2003, 44, 3945.
30. Kuo, S. W.; Chan, S. C.; Chang, F. C. Macromolecules 2003, 36, 6653.
31. Kim, B.; Lee, S. H.; Lee, D.; Ha, B.; Park, J.; Char, K. Ind Eng Chem Res 2004, 43, 6082.
32. Liu, Z. J.; Yan, D. Y. Polym Eng Sci 2004, 44, 861.
33. Zeng, H. L.; Gao, C.; Watts, P. C. P.; Kong, H.; Cui, X. W.; Yan, D. Y. Polymer 2006, 47, 113.
34. Homminga, D. S.; Goderis, B.; Mathot, V. B. F.; Groeninckx, G. Polymer 2006, 47, 1630.
35. Yang, J.; McCoy, B. J.; Madras, G. J Phys Chem B 2006, 110, 15198.
36. Chen, E. C.; Wu, T. M. J Polym Sci Part B: Polym Phys 2008, 46, 158.
37. Albano, C.; Papa, J.; Ichazo, M.; González, J.; Ustariz, C. Compos Struct 2003, 62, 291.
38. Mubarak, Y.; Harkin-Jones, E. M. A.; Martin, P. J.; Ahmad, M. Plast Rubber Compos 2000, 29, 307.
39. Xu, Y.; Gao, C.; Kong, H.; Yan, D.; Luo, P.; Li, W.; Mai, Y. Macromolecules 2004, 37, 6264.
40. Avarami, M. J Chem Phys 1939, 7, 1103.
41. Avarami, M. J Chem Phys 1940, 8, 212.
42. Cebe, P.; Hong, S. D. Polymer 1986, 27, 1183.